Access the most recent version at http://jeb.biologists.org/lookup/doi/10.1242/jeb.070755

Visuo-motor transformations involved in the escape response to looming stimuli in the crab *Neohelice (=Chasmagnathus) granulata*.

Damián Oliva[1,2] and Daniel Tomsic[2]*

1) Departamento de Ciencia y Tecnología, Universidad Nacional de Quilmes. CONICET. Argentina.

2) Laboratorio de Neurobiología de la Memoria. Depto. Fisiología, Biología Molecular y Celular, Facultad de Ciencias Exactas y Naturales. Universidad de Buenos Aires. IFIBYNE-CONICET. Argentina.

Running title: Looming detection in crabs

Key words: visual behavior, escape response, looming detection, Crustacea.

*Correspondence to: Daniel Tomsic. Laboratorio de Neurobiología de la Memoria. Depto. Fisiología, Biología Molecular y Celular, Facultad de Ciencias Exactas y Naturales. Universidad de Buenos Aires. Pabellón 2 Ciudad Universitaria (1428), Buenos Aires, Argentina. Telephone: (541) 14576-3348; Fax:(541) 14576-3447; E-mail: tomsic@fbmc.fcen.uba.ar

SUMMARY

Escape responses to directly approaching predators represent one instance of the animals' ability for collision avoidance. Usually, such responses can be easily evoked in the laboratory using two dimensional computer simulations of approaching objects, known as looming stimuli. Therefore, escape behaviors are considered useful models for the study of computations performed by the brain to efficiently transform visual information into organized motor patterns. The escape response of the crab *Neohelice (previously Chasmagnathus) granulata* offers an opportunity to investigate the processing of looming stimuli and its transformation into complex motor patterns. Here we studied the escape performance of this crab to a variety of different looming stimuli. The response always consisted of a vigorous run away from the stimulus. However, the moment at which it was initiated, as well as the developed speed, closely matched the expansion dynamics of each particular stimulus. Thus, we analyzed the response events as a function of several variables that could theoretically be used by the crab (angular size, angular velocity, etc.). Our main findings were: a) the decision to initiate the escape run is made when the stimulus angular size increases by 7˚. b) The escape run is not a ballistic kind of response, as its speed is adjusted concurrently with changes in the optical stimulus variables. c) The speed of the escape run can be faithfully described by a phenomenological input-output relation based on the stimulus angular increment and angular velocity of the stimulus.

INTRODUCTION

Collision avoidance behaviors are given particular interest in view of their biological importance. In effect, most visual animals are highly efficient in detecting and avoiding collisions, which may occur either by encounters with obstacles while they move, or by moving objects that directly approach them. Natural instances of objects approaching in collision course are the sudden attacks of predators. The maneuvers executed to evade predatory assaults are paramount behaviors that must be controlled by rather straightforward neural circuits to generate quick and reliable avoidance responses. To be effective, those responses need to be executed in a timely manner, which implies that the approaching object must be monitored in real time for the animal to decide if, when and how, to generate an escape response. Approaching objects can be effectively simulated using two-dimensional projections on a computer screen, called looming stimuli. Neurophysiological investigations in species as diverse as locust, fish and pigeons, have shown striking similarities regarding the sensory processing of looming stimuli (Rind and Simmons, 1999; Fotowat and Gabbiani, 2011; Preuss et al., 2006; Sun and Frost, 1998). However, the differences between the motor systems used by these animals to perform escape responses are enormous, raising the question of whether common sensory-motor transformation rules are exploited in species with similar sensory processing stages. Because of this, in the concluding remarks of their recent review on collision avoidance behavior, Fotowat and Gabbiani (2011) emphasized the need of comparative studies to draw general conclusions about the way in which brains process information and organize the motor outputs that allow animals to avoid collision. Unfortunately, the number of animal models that proved to be suitable for behavioral as well as neuronal analysis of responses to looming stimuli is still scarce.

In a previous paper, we introduced a new experimental model using the crab *Neohelice granulata*, which offers good opportunities for investigating the processes of looming detection, escape decision and motor control at both behavioral and neuronal levels (Oliva et al., 2007). Briefly, in its natural environment this crab is predated by gulls, and consequently, reacts to the image of an approaching object by running away in the opposite direction. The escape response can be readily elicited in the laboratory using looming stimuli and accurately measured with a treadmill-like device. In addition, the response of identified neurons from the lobula (third optic neuropile of arthropods), some of which responded to looming stimuli in a way that parallels behavior, can be electrophysiologically recorded in vivo (Berón de Astrada and Tomsic, 2002; Medan et al., 2007; Oliva et al., 2007; Sztarker and Tomsic, 2008).

Avoidance responses to looming stimuli range from ballistic-like kind of behaviors to more complex ones where the response is continually adjusted while being performed according to the observed changes in the approaching stimulus direction and speed. The first types of responses,

which can be described as single threshold response systems, are triggered when an optical variable of the image exceeds certain value, after which the animal displays a stereotyped behavior. This type of responses has been described in species such as crayfish (Glantz, 1974) and fish (Preuss et al., 2006). In other cases, the avoidance response is composed of distinctive preparatory stages, each one being triggered when an optical variable reaches a particular theshold. Examples of this multistage kind of response can be found in the fly (Tammero and Dickinson, 2002; Card and Dickinson, 2008ab), crabs (Hemmi and Pfeil, 2010), and in the locust (e.g. Santer et al., 2005ab, 2006, 2008; Gray et al. 2006; Fotowat and Gabbiani, 2007; Fotowat et al., 2011). Finally, there are avoidance responses that are continuously adjusted to external changes, such as those occurring during unpredictable modifications in the trajectory or velocity of predatory attacks. These responses can be described as continually regulated systems. Behaviors guided by continued regulated systems have been mostly studied in the context of animal navigation (e.g. Srinivasan et al., 2000; Fry et al., 2009), but not as much in the context of predator avoidance (Land and Layne, 1995).

Our previous characterization of the response to a single looming stimulus in the crab (Oliva et al., 2007), has provided some indications that this behavior would consist of a threshold-type decision for initiating the escape run, followed by a visually regulated mechanism for continually controlling the velocity of the escape run. Here, we evaluated this hypothesis by analyzing the responses of crabs to a wide variety of looming stimuli that differed in size and approaching velocity. The analysis led us to the identification of the optical stimulus' variables that the animal most likely takes into account to perform the behavioral response. Moreover, we propose a phenomenological input-output relation based only on these variables that allow us to predict the behavioral performance to the different dynamics of approaching objects.

MATERIALS AND METHODS

Animals:

Animals were adult male *Neohelice granulata* (previously *Chasmagnathus granulatus*) crabs 2.7–3.0 cm across the carapace, weighing approximately 17 g, collected in the rías (narrow coastal inlets) of San Clemente del Tuyú, Argentina, and transported to the laboratory, where they were lodged in plastic tanks (35 cm, 48 cm, 27 cm) filled to 2 cm depth with diluted seawater at a density of 20 crabs per tank. Water used in tanks and other containers during the experiments was prepared using hw-Marinex (Winex, Hamburg, Germany), salinity 10–14‰, pH 7.4–7.6, and maintained within a temperature range of 22–24°C. The holding and experimental rooms were maintained on a 12h:12h light:dark cycle (lights on 07.00h to 19:00h) and the experiments were run between 08.00h and 19:00h. Experiments were performed within the first 2 weeks after the animals arrived. Crabs

were fed rabbit pellets (Nutrients, Buenos Aires, Argentina) every 3 days and after feeding the water was changed. Following experiments, animals were returned to the field and released in a location separated by 30 km from the capture area.

Visual stimuli and behavioral recording setup

Computer-generated visual stimuli can be projected either simultaneously or alternatively on five flat screen monitors (Phillips 107T; horizontal and vertical screen dimensions were 32 cm by 24 cm respectively, refreshing rate 60 Hz), located at 20 cm in front, back, above and on both sides of the animal (Oliva et al., 2007). The monitors were covered with anti-glare screens to reduce reflections between them. All visual stimuli were generated with a PC using commercial software (Presentation 5.3, Neurobehavioral Systems Inc., Albany, CA, USA). Since in this study we were particularly interested in investigating the response initiation and running speed, the experiments were performed with stimuli presented only on the monitor located at the animal's right; in order to keep the image of the approaching stimulus at a fixed position on the lateral pole, as the crab runs sideways (Land and Layne, 1995). We have previously shown that the initial response time is the same for stimuli approaching frontally or laterally (Oliva et al., 2007). However, when the stimulus is approaching frontally, the escape response includes an initial rotational component that allows the animal to run sideway. This rotation maneuver makes the analysis of the run velocity more difficult, a complication that we wished to avoid at this stage. Besides, stimuli appearing from the lateral pole are seen by the animal monocularly, which made our results comparable with those obtained in locusts and pigeons (reviewed in Rind and Simmons, 1999; Fotowat and Gabbiani, 2011).

The effectiveness of 2D computer images to elicit the crab's escape response has been already shown (Oliva et al., 2007). Moreover, in recent experiments we found no differences between the escape response elicited by a black sheet of cardboard approaching the animal and the computer simulation of an object of the same size and speed of approach (Oliva, 2010).

The locomotor activity of the crab was investigated in a walking simulator device that has been described in detail elsewhere (Oliva et al., 2007). Briefly, it consisted of a floating styrofoam ball that could be freely rotated by the locomotor activity of an animal, attached in a standing position to a weightless rod through a piece of rubber glued to its dorsal carapace. The rod was introduced inside a metal guide, positioned vertically above the ball, where it could slide up and down with little friction (Fig. 1A). This allowed the animal to feel its own weight and thus adopt its natural posture while performing on the ball. The rod and guide both had square sections, which prevented rotational movements and thus assured that the animal always saw the stimulus with the same side of the eye (the lateral pole in this study). The styrofoam ball (16 cm in diameter) floated within a bowl-shaped container partially filled with water. Horizontal displacements of the ball were prevented by four set points provided by two optical mice and by two flexible sheets located at right

angles from each other. The rotation of the ball was recorded by the two mice, with their optical reading systems protected by transparent acetate sheets, which also guaranteed the smooth movement of the ball. Locomotion signals were acquired using the recording facilities of the same commercial software that generated the visual stimuli. Mice data were taken at each frame update (16.7 ms), which assured an accurate correspondence between the recorded response times and the stimulus features (size, border speed, etc). Two Presentation programs were run in two separate PCs. The PC that generated the visual stimuli (PC1) was used to record one of the mice, and to trigger the recording by the second mouse in the second PC (PC2). Hence, the program that generated the visual stimulus synchronized the recording of the two mice just before stimulus onset. The data from mice 1 and 2 during a trial generated two Presentation files, which contained a list of times associated with each data record and frame update. Further detail on data recording and analysis can be found in Oliva et al. (2007). Behavior was also monitored by visually observing the animal on-line through a video camera.

Kinematics of object approach

The stimuli used simulated dark squares of various sizes approaching with constant speeds on a direct collision course to the animal (Fig. 1B). Let l denote the object half-size. The distance between the animal eye and object at time t is $x(t)$ and the object subtends an angle $\theta(t)$ on the eye. Thus, we can write:

$$\tan(\theta(t)/2) = \frac{l}{x(t)} \qquad \text{Eqn 1}$$

With the chosen coordinates system and time definitions, we have $x(t) \geq 0$, $t \geq 0$. Objects were simulated to start their approach from a distance L = 5 m. The position of the object is defined by:

$$x(t) = L - v \cdot t \qquad \text{Eqn 2}$$

Where v, is the absolute value of the approach speed.

The square drawn on the monitor screen (Fig. 1B) has a half-size $l_{screen}(t)$ and depends on the distance from the monitor to the eye of the animal $x_{eye\text{-}screen}$, as follows:

$$\tan(\theta/2) = \frac{l_{screen}}{x_{eye-screen}} = \frac{l}{x(t)} \qquad \text{Eqn 3}$$

Replacing $x(t)$ from Eqn 2, and solving for $l_{screen}(t)$ we get:

$$l_{screen}(t) = \frac{x_{eye-screen} \cdot l}{x(t)} = \frac{x_{eye-screen} \cdot l}{L - v \cdot t}. \qquad \text{Eqn 4}$$

Eqn 4 describes a half-size square drawn on the screen monitor as a function of time. Due to the limits imposed by the screen's size and distance to the animal's eye, maximum stimulus expansion was $\theta(t)=60^{o}$.

In the literature regarding looming detection the dynamic of a stimulus expansion is usually characterized by the relation *l/v* (Gabbiani et al., 1999). By replacing *x(t)* from Eqn 2 in Eqn 3 we get:

$$\tan(\theta/2) = \frac{l}{L - v \cdot t} = \frac{1}{L/l - v \cdot t/l} = \frac{1}{1/\tan(\theta_0/2) - t/(l/v)} \qquad \text{Eqn 5}$$

From Eqn 5 it can be observed that in the present study each stimulus is characterized by a value of *l/v* and of θ_0.

Stimuli used

We used a total of 8 stimuli (Table 1). For stimuli 1-4 we maintained the approach speed *v*=142.5 cm/s and varied the size *l* from 8.5 cm to 64 cm. The subtended angle of the smallest stimulus at the initial distance was 1.8°, which is well above the sampling resolution of the crab's eye. In fact, in the lateral part of the eye the resolution reaches values between 0.83 and 1.2 cycles/deg, corresponding to interommatidial angles between 0.6° and 0.4° respectively (Berón de Astrada et al., 2012). Thus, animals would not have optical limitations to detect differences between initial sizes of the smaller stimuli used here. For stimuli 5-8 we kept *l*=17 cm and varied *v* from 35.5 cm/s to 286 cm/s. These speeds tried to simulate predators that approach the animal faster than its ability to run away (*Neohelice's* highest escape speed is 35 cm/s). Moreover, this minimized the compensation of the stimulus growth by the animal's speed developed while attempting to get away. Stimuli 2 and 7 had the same size and expansion dynamics, hence, they were indistinguishable by the animal from each other. The similarities in the results obtained with them served as an internal control for each experimental series.

Conditions of stimulation

In Oliva et al. (2007) we described some important features of the escape response and optimal stimulation parameters such as interval between trials, the direction of approach and object contrast against the background. Based on those results, we began stimulation after the animal had remained visually undisturbed for 10 min inside the setup. In all trials the stimulus remained stationary for 30 s at its initial position before starting to increase in size. The inter-trial interval was set to 3 minutes to reduce habituation and fatigue effects (Fig. 5 in Oliva et al., 2007). Stimuli were applied only from the right to reduce variability (Fig. 6 in Oliva et al., 2007). We used black squares expanding on a white background (Fig. 10 in Oliva et al., 2007). Radiance on the monitor screen was 4 mW/m^2 (black square) and 240 mW/m^2 (background). The eight stimuli in Table 1 were applied to each animal in a random order, and only once.

Animal and response selection

All the animals challenged with the looming stimulus in the present study consistently displayed escape responses. In some trials animals were walking when the expansion started. Results of ongoing experiments suggest that this does not affect response initiation times. However, to simplify the analysis, we used only those trials where the animals were motionless before the beginning of the expansion (>85% of trials). Additionally, we excluded those responses in which the traveled distance during the expansion was below 10% of the mean response for that stimulus (this corresponded to less than 5% of responses).

Criteria for the beginning of the escape response

We defined the beginning of the escape run as the moment in which the recording trace showed the animal's first movement after the expansion of the image had initiated. This first stepping movement is easily detected and is characteristically followed by a progressive increase in the animal's speed (see Fig. 4 in Oliva et al. 2007, and Fig. 3A in this article). The time of escape t_{esc} then corresponded with the time interval between the beginning of the stimulus expansion ($t = 0$) and the moment when the animal initiated the escape. Each trace was examined separately and t_{esc} was obtained for every trial in all the animals.

Data analysis

To estimate the animal's speed we convolved the instantaneous speed with a 100 ms square window and normalized the resulting waveform (Gabbiani et al., 1999). Least squares regressions of the animal's speed with respect to stimulus optical variables described later in the results were used to fit the input-output relation between these variables and the escape speed. The Kruskal–Wallis test (KWT) was used to compare the medians of samples across different stimuli. Unless otherwise stated, the p values were derived from the KWT. When no significant differences were found we report average values across treatments. To analyze the visuomotor delay we computed the Pearson correlation coefficient between different kinematic variables with the parameters l/v and θ_0 (Table 1) at a fixed processing delay δ before escape (Fotowat and Gabbiani, 2007). Data analysis procedures were written in Matlab (TheMathWorks). Further procedures are explained in the results section.

RESULTS

The aim of the present study was to identify which optical variable in a looming stimulus (e.g. angular size, angular velocity) is first used by the crab to decide to begin an escape run and, second, to regulate its speed. In other words, we expected to find a variable and a mathematical function that

would allow us to predict the initiation and speed of the response to looming stimuli. This required the analysis of responses to different stimulus sizes and speeds of approach, thus exhibiting distinct expansion dynamics, and the search for the threshold value of an optical variable common to all stimuli at the time that a particular behavioral event occurred (e.g. when the escape response started or when the crab ran at a particular speed).

Fig. 2 shows the mean responses of a group of 20 crabs to the 8 looming stimuli that were used in this study (Table 1). Because all stimuli approached from the same side, the responses were highly directional (Fig. 6 in Oliva et al. 2007). The temporal course of the responses was as follows: animals were initially motionless and remained so even when the stimulus had begun its expansion. Suddenly they started running in the opposite direction to the stimulus (arrows in each trace mark the mean escape time, t_{esc}). Statistical differences between the mean t_{esc} of stimulus 1 and 2 (arrow below the pink and red trace respectively, p <0.05), indicates that animals were able to distinguish between the smaller stimulus sizes used in this study. After the initial movement, the animals gradually increased their speed as the object grew larger, as if they were "tracking" the object over its approach until the expansion was completed, after which speed was suddenly reduced. For all stimuli, we found the same response stages previously described for a single stimulus (Oliva et al., 2007). Individual responses can be observed in Fig. 3A of this paper and in Figs. 3 and 4 of Oliva et al. (2007).

Optical variables that may predict the onset of escape run

We assumed that crabs made the decision to initiate the escape from looming stimuli based on threshold criteria, i.e. the escape began after a certain optical variable had reached a particular value. The analysis therefore sought to identify a variable with a common value for all the stimuli at the moment the animal made the decision to escape. In our analyzes we took into consideration several optical variables Z (Table 2) that the crab could compute to decide the escape, some of which have been shown to be important in studies with different animal species (see Introduction). The following is a description of these variables. All of them are described at t_{esc}-δ, where δ is the delay between the animal decision for escape and the actual behavioral measurement (see below).

Time elapsed since the beginning of the expansion. The animal begins the escape a fixed time after detecting the beginning of the expansion. We called this variable: $Z_1=t_{esc}-\delta$.

Time to collision: Some animals (e.g. pigeons) have neurons that are activated a fixed time before the collision occurs (Wang and Frost, 1992). Therefore we measured the time to collision t_c, δ milliseconds before the escape and named this variable: $Z_2=t_c(t_{esc}-\delta)$.

Angular size, angular velocity or angular acceleration: Some animals produce collision avoidance responses when the angular size of the stimulus has reached a threshold (Fotowat and Gabbiani, 2007). Angular velocity (Hemmi 2005b) or angular acceleration, are two other alternatives that might

be taken into consideration. Therefore, we evaluated angular size $Z_3=\theta(t_{esc}-\delta)$, angular velocity $Z_4=\dot{\theta}(t_{esc}-\delta)$, and angular acceleration $Z_5=\ddot{\theta}(t_{esc}-\delta)$.

Angular Increment: Finally, animals might consider the angular increment which we named $Z_6=\Delta\theta(t_{esc}-\delta)=\theta(t_{esc}-\delta)-\theta(t_{=}0)$. The crayfish defensive reflex occurs when the angular size of the approaching object increases by 8 degrees (Glantz, 1974).

Time delay between the decision and the measurement of the escape

Once the decision to initiate the escape has been made, additional time is required for the behavior to occur, such as the time consumed in conveying the message downstream through the neural system and to the muscles, and to generate the forces necessary to move the legs and overcome the inertia of the recording device. Consequently, the optical variables must be analyzed in a time t_{esc}-δ, where δ is the delay between the moment the animal decided to escape and its associated motor response (see Fig. 3B). The magnitude of δ is then crucial for ascertaining the value attained by the optical parameters at the time of the escape decision. An error in the value of δ would render differential errors in the values of the optical variable associated with the escape decision for the different looming stimuli. Thus, we were required to measure the magnitude of δ as precisely as possible. For this reason we performed an experiment where we challenged the animals with a visual stimulus that could be taken as a threat as soon as it appeared, consisting of a black edge spanning 60° in elevation that progressed horizontally from one side to the other of the lateral monitor (see inset on Fig. 4). Unlike approaching objects, which usually begin subtending a small angular size that does not provoke an escape until growing up to some extent, a large visual stimulus moving fast enough would be interpreted as an immediate danger, thus instantly prompting an escape response. Therefore, the delay between the visual input and the motor output for this stimulus likely corresponds to the minimal latency obtained between the onset of stimulus motion and the onset of escape. Fig. 4 shows the latency of the escape response as a function of the angular velocity of stimulus' tangential motion. The delay was about 1 second at low angular velocities (20°/s), but was reduced gradually to an asymptotic minimum value of 170 ms for angular velocities of 180 °/s and beyond. From this experiment we concluded that the delay between visual input and behavioral measurement of the escape was *170±25 ms* (mean±s.e). The decision, however, can not be thought to occur just as the visual stimulus reaches the retina, but at a deeper brain level. A substantial amount of evidence suggests that the decision to escape from visual stimuli may arise at the level of the giant neurons of the lobula (e.g. Tomsic et al., 2003; Sztarker and Tomsic, 2008, 2011), which present a response delay to visual stimuli of about 35 ms (Medan et al., 2007). This time has to be subtracted from the visual input to motor output delay calculated above in order to obtain a realistic estimation of the elapsed time between the decision making process and the actual escape recording. Therefore, $\delta=170-35=135$ *ms*.

What optical variable best predicts the onset of escape run?

All optical variables were measured at t_{esc}-δ in every trial for each animal. We then analyzed whether any of the variables $Z_{1\text{-}6}$ attained a constant value for all the stimuli at the moment the animals decided to initiate their escape run. Fig. 5 shows the results. Of the six variables analyzed, *angular increment* was the only one whose value remained constant throughout the stimuli (p = 0.6). All the other variables did not meet this criterion and presented significant differences among the stimuli (p <0.001). Therefore, we concluded that the escape is initiated when *angular increment* exceeds a value of approximately 7 ± 0.3 degrees (mean ± s.e) (dashed line in Fig. 5F).

The previous analysis was made with the δ value derived from experiments using a translating stimulus (Fig 4). It could be argued that the effective delay used by the crab for approaching stimuli may not be the same than the one used for translating stimuli, thus casting doubts on our conclusions. Therefore, we performed a different analysis to test whether *angular increment* or any other kinematic stimulus variable was equal to a constant threshold at a fixed delay before escape initiation. This analysis, used by Fotowat and Gabbiani (2007) to identify the optical variable best related to the locust takeoff time upon looming stimuli, allows to determine the delay directly from the experimental data obtained with the looming stimuli. According to this analysis, a necessary condition for *angular increment* to be constant at a certain delay before escape initiation is that its correlation coefficient with l/v be zero at that delay. Therefore, we systematically computed the correlation coefficient between *angular increment* and l/v as a function of time before escape (Fig. 6, blue curve). In the case of *angular increment*, the correlation coefficient was zero around 140 ms before escape initiation time. This estimation of the delay resulted in close agreement with that obtained experimentally by using translating stimuli (135 ms). Furthermore, the analysis based on the correlation coefficients clearly shows that *angular increment* is the only kinematic stimulus variable that crosses the zero correlation level within the time window expected for a functional delay. Because our stimuli are characterized by l/v but also by θ_0, we checked if for 140 ms delay the *angular increment* also showed a zero correlation coefficient with θ_0. The analysis revealed that in fact, with 140ms delay, the correlation value is not significantly different from zero (ρ=-0.10±0.14, 95 % confidence intervals estimated using the bootstrap method)(Wasserman 2004).

The two different methods of analysis described above led us to the same conclusion: crabs make the decision to initiate the escape when the stimulus angular increment reaches 7 degrees (Fig. 5F).

The escape run is under continuous visual regulation.

In many animals, the escape behavior to predator attacks often represents a ballistic movement (e.g. the crayfish tailflip: Linden and Herberholz, 2008; the C start escape response of

fish: Preuss et al., 2006). Thus, once the response has been launched it goes to completion without adjustments related to changes in the eliciting stimulus. This does not seem to be the case for the crab's escape run. To investigate the dependency of the escape response on the incoming visual information, we performed an experiment using the same looming stimulus, but we stopped it at different stages of its growth. Fig. 7 shows that immediately after the stimulus finished growing the escape run always decelerated. The result clearly shows that the escape run is under continuous visual regulation, rather than ballistic.

An Input-Output relation for the regulation of the animal escape speed.

The result of Fig. 7 shows that the crab is sensing the stimulus expansion continually and adjusts the motor output accordingly. Moreover, a cursory inspection of Fig. 2 suggests that the escape speed of the animals is related to the dynamics of the stimulus expansion. In fact, those stimuli presenting fastest expansion dynamic (corresponding to the smaller or the faster approaching objects of the series) exhibited the steepest gain of escape speed, whereas those presenting the slower expansion rate (corresponding to the larger or slower approaching objects) resulted in more gradual speed changes. Therefore, it is quite apparent that crabs adjust their speed as a function of the image expansion rate. We then attempted to find a phenomenological *Input-Output relation* (f_{IO}) that depended only on one of the optical variables of the looming stimuli $Z_{1\text{-}6}(t)$ to describe the animal's escape response. Ideally, this function should be able to describe the condition when animals are still ($v_c(t)=0$) as well as the changes in speed after escape initiation. The relationship between the speed of the crab v_c, the optical variable Z, and the input-output relation is given by: $v_c(t)=f_{IO}[Z(t-\delta)]$. A description of this type implies searching for different potential optical variables Z and f_{IO} functions. Among the optical variables Z described in Table 2, the only one that could describe the entire escape response (both the initiation and the speed of the escape run) is the variable $\Delta\theta$ (remember that the escape run starts invariably when $\Delta\theta$ reaches a threshold value of $\Delta\theta_{esc}$=7º). Therefore, we incorporated $\Delta\theta$ in our description, as it is the optical variable that best predicts whether the animal is at rest or escaping. Our first approach was to extend the prediction on escape initiation to escape speed by using $\Delta\theta$ only. To write this hypothesis mathematically, we defined the variable $u_1(t-\delta)=\Delta\theta(t-\delta)-\Delta\theta_{esc}$ to fulfill: If $\Delta\theta<\Delta\theta_{esc}$, then u_1 is negative and the animal remains still. If $\Delta\theta\geq\Delta\theta_{esc}$, then u_1 is positive and the animals escape with speed $v_c(t)>0$.

In Fig. 8 we illustrate our analysis using a hypothetical case. Fig. 8A shows the angular increment $\Delta\theta$ as a function of time and Fig. 8B shows the variable $u_1(t-\delta)$. The variable u_1 is obtained by moving down the variable $\Delta\theta$ at a fixed $\Delta\theta_{esc}$ value (note the difference in the y axis scale). This determines two regions separated by the black horizontal dashed line: for values of u_1 below the line the animal would decide to remain motionless (exemplified by the blue circle). When u_1 intercepts the line the animal would decide to initiate the escape (green circle), and for greater u_1 values the

animal would decide to escape (red circle). Once u_1 has been defined we need to propose a possible function f_{IO} to describe the speed of the animals. For this, it is important to take into account that animals operate with motor and sensory processes that have saturation limits (Blickham and Full, 1987; Gabbiani et al. 1999). These limits constrain the performance of the animal and, hence, must be considered in a description of the escape speed. We propose :

$$v_c = f_{IO}(u_1) = v_{1,\max} \cdot \frac{u_1}{u_{1,50\%} + u_1} \qquad \text{if} \quad u_1 \geq 0. \qquad \text{Eqn 6}$$

$$v_c = f_{IO}(u_1) = 0 \qquad \text{if} \quad u_1 < 0.$$

This saturating function is described by the parameters $v_{1,max}$ and $u_{1,50\%}$. The parameter $v_{1,max}$ corresponds to the maximum speed the animal can reach and the parameter $u_{1,50\%}$ is the value of the variable u_1 when the animal reaches 50% of $v_{1,max}$. Fig. 8C shows the function f_{IO} and the geometric representation $v_{1,max}$ and $u_{1,50\%}$. Another important parameter to characterize f_{IO} is with its slope at $u_1=0$. The slope, called m_1, depends on $v_{1,max}$ and $u_{1,50\%}$ as follows: $m_1 = v_{1,max} / u_{1,50\%}$ (Fig. 8C). m_1 will be used later to compare responses to the different stimuli. Fig. 8 then, shows step by step how we obtained a prediction of the animal's speed $v_c(t)$ using the f_{IO} function: 1) We started with a stimulus value of $\Delta\theta$ (Fig. 8A). 2) We calculated $u_1(t-\delta)=\Delta\theta(t-\delta)-\Delta\theta_{esc}$ (Fig. 8B). 3) We introduced the value of $u_1(t-\delta)$ in f_{IO} (black curved dashed arrow from Fig. 8B to Fig. 8C) to calculate the crab's speed $v_c(t)=f_{IO}[u_1(t-\delta)]$ (vertical arrows in Fig. 8C). 4) Finally, we obtained the speed predicted by f_{IO} as a function of time (horizontal arrows from Fig. 8C to Fig. 8D).

Fig. 9A shows examples of speed fits using the f_{IO} of Eqn 6 for the eight stimuli in a single crab. We fitted individual records (N = 20 animals, 8 stimuli per animal) for the time interval ranging from t_{esc} to the end of the expansion. For each record we determined t_{esc} as explained in the methods. Then we obtained $\Delta\theta_{esc}$ and u_1. Finally, we determined f_{IO} parameters ($v_{1,max}$, $u_{1,50\%}$ and m_1) by least-square fits in each record. After obtaining the f_{IO} parameters for all trials, we tested whether each of these values was the same or they differed among the different stimuli (Fotowat and Gabbiani, 2007). As for escape initiation, common values mean that with the proposed f_{IO}, using u_1 alone, we could predict the speed of each crab with independence of the stimulus applied. However, Fig. 9B-C shows that the values of $v_{1,max}$, $u_{1,50\%}$ and m_1 , are significantly different among stimuli ($p \leq 0.01$ for the three parameters). Therefore, the proposed function failed to describe the escape response.

An inspection of Fig. 9D, reveals that m_1 is highest for stimuli with the fastest expansion dynamics (stimulus 1 and 8). This suggests that the angular velocity of the stimulus affects the speed of the escape response. In fact, angular velocity $\dot{\theta}(t)$ is an optical variable central to those models describing the response of looming sensitive neurons in different animal species (e.g. locust: Hatsopoulos et al., 1995; Gabbiani et al., 2002; pigeons: Sun and Frost, 1998). The simplest operation available to include angular velocity in our description of the crab's escape response would

be to add it to the stimulus angular increment in the form $u_2(t) = u_1(t)+\beta\cdot\dot{\theta}(t)$, where β is a proportionality constant. But, because $\dot{\theta}(t)$ has a positive value from the very beginning of the stimulus approach, this $u_2(t)$ does not satisfy the requirement of crossing the zero value when the decision to escape is made (see Fig. 5D).

Another way of including the stimulus' angular velocity would be as a multiplicative factor. In fact, a multiplicative computation proved to be performed by visual neurons sensitive to looming (Gabbiani et al., 2002). We then propose a new variable $u_2(t)$ that incorporates the angular velocity $\dot{\theta}(t)$ as a product:

$$u_2(t) = u_1(t)\cdot\dot{\theta}(t) = (\Delta\theta(t) - \Delta\theta_{esc})\cdot\dot{\theta}(t) \qquad \text{Eqn 7}$$

This proposal is justified as: 1) $u_2(t_{esc}-\delta)=0$ when the escape initiates, because $u_1(t_{esc}-\delta)=0$, as shown before; 2) the product of $u_1(t)$ and $\dot{\theta}(t)$ results in a greater reduction of m_1 for those stimuli with the fastest expansion dynamics, which contributes to cancel out the differences in the slopes obtained with the former variable $u_1(t)$ (Fig. 9D, stimulus 1 and 8).

Fig. 10A shows examples of speed fits using the f_{IO} of Eqn 7 for the eight stimuli in a single crab. Following the procedure described above, but now using Eqn 7, we obtained $v_{2,max}$, $u_{2,50\%}$ and m_2 in every trial and evaluated their independence. Fig. 10B-D shows that, indeed, but now using the variable $u_2(t)$, the parameters $v_{2,max}$, $u_{2,50\%}$ and m_2 do not differ significantly among the stimuli ($v_{2,max}$: p =0.4 ; $u_{2,50\%}$: p =0.7 ; m_2 : p = 0.5). These results suggest that we have found a phenomenological input-output relation entailing the product of the stimulus angular increment $\Delta\theta$ and the angular velocity $\dot{\theta}$, which successfully predicts the escape performance upon a wide variety of looming stimuli.

The following equations summarize our visuo-motor tranformation model of the crab's escape performance.

$$u_2(t) = u_1(t)\cdot\dot{\theta}(t) = (\Delta\theta(t) - \Delta\theta_{esc})\cdot\dot{\theta}(t)$$

$$v_c(t) = f_{IO}\left[u_2(t-\delta)\right] = v_{2,\max}\cdot\frac{u_2(t-\delta)}{u_{2,50\%}+u_2(t-\delta)} \qquad \text{if } u_2(t-\delta)\geq 0 \qquad \text{Eqn 8}$$

$$v_c(t) = 0 \qquad \text{if } u_2(t-\delta) < 0$$

Fig. 11 shows the animals' speed as predicted by Eqn 8, superimposed to the mean speed of the group of crabs (N= 20) of Fig. 2. The prediction was made by estimating the values of $\Delta\theta_{esc}$, $v_{2,max}$ and $u_{2,50\%}$ as follows: $\Delta\theta_{esc}$=7º was the mean data value of Fig. 5F, whereas $v_{2,max}$ =17 cm/s,

$u_{2,50\%}$ =490 deg^2/s and m_2=0.035 cm/deg^2 were the mean values in Fig. 10B,C,D. The good matching between the predicted and the actual mean speed of crabs for all the stimuli tested indicates that the fits performed with these optical values are largely satisfactory.

DISCUSSION

The relevance of studying the mechanisms by which animals detect approaching objects and avoid collisions is well recognized (see reviews of Rind and Simmons, 1999; Fotowat and Gabbiani, 2011). Studies in pigeons revealed that specialized visual neurons carry out several different computations in parallel to analyze signals from approaching objects such as predators (Sun and Frost, 1998), indicating that information to avoid collisions can be achieved in different ways (Laurent and Gabbiani, 1998). On the other hand, the motor network and muscular machinery for generating escape behavior in animals like pigeons, fish, locusts or crabs are largely different. Thus, comparative studies have been called for to understand how sensory-motor integration contributes to decision making in the context of collision-avoidance behaviors and learn whether common sensory-motor transformation rules are exploited by different species (Fotowat and Gabbiani, 2011).

In a previous study we introduced the crab as a new model to study collision-avoidance behaviors. We have shown that the behavior of crabs upon the sight of a predator attack happening in the wild, can be reliably elicited and thoroughly measured in the laboratory using 2D computer simulations and a treadmill-like device. We also showed that identified neurons of the lobula (similar to those studied in the locust) that seem to play a central role in this behavior can be recorded in the living animal (Oliva et al., 2007). Therefore, crabs emerge as an attractive model to contribute to our understanding of the processes involved in collision avoidance behaviors.

In the present study we performed a systematic behavioral analysis of responses to a wide variety of looming stimuli to identify which parameters are used by the crab to initiate an escape run and to determine its speed. The main findings can be summarized as follows: a) the decision to initiate the escape response is made on fixed criteria, i.e. when the angular size increases by 7˚ (Fig. 5F). b) The escape run is not a ballistic all or none kind of response, because its speed is adjusted concurrently with changes in the stimulus optical variables (Fig. 2 and 7). c) The escape performance can be faithfully predicted (Fig. 11) by a phenomenological input-output relation depending on a multiplicative operation of the stimulus angular increment and angular velocity (Eqn 8).

The decision to initiate the escape run

A central issue regarding avoidance responses to approaching objects is knowing which one of the various optical parameters of the expanding image is used by the animal to decide when to

start the response. Coincidently with our present results in *Neohelice*, studies in other crustacean have shown that the decision is made based on an increase in the apparent size of the stimulus. For instance, the critical stimulus parameter to initiate the escape run in the crab *Heloecius* was found to be an increase of 5.6˚ (discussed in Hemmi, 2005b), whereas in the crayfish the required increase was about 8˚ (Glantz, 1974). In a previous study using a single looming stimulus we reported that *Neohelice (=Chasmagnathus)* started the escape when the angular size of the stimulus has grown approximately by 10˚(Oliva et al., 2007), which is 3˚ above the angular increment reported here. This discrepancy comes from the fact that in our previous study we did not take into account the delay time between the visual stimulus and the response recording, as was considered in the present study (Fig. 3). The present value of $\Delta\theta_{esc}$=7º is in perfect agreement we those reported for *Heloecious* and crayfish.

On the other hand, studies with fiddler crabs performed in the field by Hemmi and colleges depicted a different scenario (Hemmi, 2005ab; Hemmi and Pfeil, 2010). These studies showed that the escape response to an approaching dummy predator includes different stages, each of which would be triggered by a different parameter of the visual stimulus. For instance, retinal speed may lead to an initial freeze followed by a run towards the burrow entrance, where the crab may stay and assess for an increase in the stimulus' apparent size before deciding to descend into the burrow. The progression along these different response stages has been related with an escalation of the predation risk imposed by the stimulus closeness (Hemmi, 2005a). These field studies in fiddler crab have been carried out using a dummy that always approached the crabs with variable deviations away from the collision course. Such stimuli would stand for a lower risk than a similar one that approaches the crab directly. Surprisingly, however, the indirect stimulus elicited earlier responses than the direct one. This is because, at a long distance, an object moving tangential to the crab generates greater retinal motion than a pure looming stimulus, which can be used by the animal to perform an earlier kind of startle response (for a discussion of this apparent paradox see Hemmi, 2005ab). In contrast with these field studies, our laboratory experiments enabled us to disentangle the looming stimulus from any translational motion component, and therefore to investigate the computations underlying the detection of visual stimuli approaching on direct collision course to the animal.

The regulation of the escape speed

In crabs, the escape behavior to visual stimuli is far from a simple reflex, but rather a finely tuned, complex behavioral sequence that is modulated at all levels of organization (for a review on this subject see Hemmi and Tomsic, 2011). Therefore, our finding that crabs continuously adjust their escape speed according to ongoing information provided by the visual stimulus (Figs. 2 and 7), is not surprising. However, the possibility of measuring the changes in the speed of the escape run and

relating them to concurrent changes in the stimulus optical parameters offers a remarkable opportunity for studying the visuo-motor transformation underlying a non-ballistic kind of behaviour. Early studies of Wiersma and collaborators on crustaceans revealed the existence of neurons sensitive to different types of visual motion (reviewed in Wiersma et al., 1982). More recently, we identified a few classes of lobula giant (LG) neurons that are highly sensitive to looming stimuli (Medan et al., 2007; Oliva et al., 2007). Moreover, we showed that the firing rate of these neurons increases with the stimulus angular expansion, in a way that appears to anticipate the animal's speed of run (Fig 9 in Oliva et al., 2007). That study, however, was performed using a single looming stimulus, which precluded making quantitative analyses relating the stimulus' expansion dynamics to the LG neurons' firing rates, and of these with the animals' speed. The results presented here will make it possible to investigate these relations. We are currently recording the response of the LGs to the full set of looming stimuli used in the present study. Our preliminary results indicate that the LGs may indeed play a central role in the visuo-motor transformations occurring during the escape response to approaching objects in the crab.

Behavioral studies in simplified laboratory conditions and the complexity of the real world

An animal behaving in its natural environment has to relentlessly make behavioral decisions based on the flow of incoming information and on its previous experience. Although at first sight the crab's avoidance response to an approaching predator may appear as a simple reflex behavior, this is clearly not the case. Upon detection of the approaching stimulus, crabs, like many animals, have to decide whether, when, in which direction, and how intensely to perform an escape response. Each one of these decisions is known to be strongly affected by environmental and behavioral contexts, such as the animal's position relative to a refuge and by the animal's learnt experiences (Hemmi and Tomsic, 2011). But if the environment is so important in shaping the avoidance behavior, what can we learn about the results from studies performed in simplified and rather artificial laboratory conditions? The answer is straightforward. As long as the essence of the behavior is preserved, we can use the well controlled stimulation conditions to investigate the fundamental features of the response. Characterizing the response to simple stimuli is a requisite for identifying neurons important for such behavior, and for understanding the way these neurons perform their fundamental operations.

ACKNOWLEDGEMENTS

We thank M. Berón de Astrada, V. Medan, F. Magani, S. Nemirovsky, and G. Hemitte for fruitful discussions and corrections to this manuscript. This work was supported by posdoctoral fellowships from the National Research Council of Argentina (CONICET) to D. O at National

University of Quilmes, and from the following research grants to D.T.: Universidad de Buenos Aires, grant number 01/W888; ANPCYT, grant number PICT 2010-1016.

582 **REFERENCES**

583

584 **Berón de Astrada, M. and Tomsic, D.** (2002). Physiology and morphology of visual movement
585 detector neurons in a crab (Decapoda: Brachyura). *J Comp Physiol A* **188** (7), 539-51.
586 **Berón de Astrada, M., Bengochea M., Medan V. and Tomsic D.** (2012) Regionalization in the eye
587 of the grapsid crab *Neohelice granulata (=Chasmagnathus granulatus)*: variation of resolution
588 and facet
589 diameters. *J Comp Physiol A.* **198**:173–180.
590 **Blickham, R. and Full, R. J.** (1987). Locomotion energetics of the ghost crab. II. Mechanics of the
591 center of mass. *J. exp. Biol.* **130**, 155–174.
592 **Borst, A. and Bahde, S.** (1988). Visual information processing in the fly's landing system. *J Comp*
593 *Physiol A.* **163**, 167-173
594 **Card, G. and Dickinson, M.** (2008a). Visually mediated motor planning in the escape response of
595 Drosophila. *Curr Biol.* **18:**1300-1307.
596 **Card, G. and Dickinson, M.** (2008b). Performance trade-offs in the flight initiation of Drosophila. *J.*
597 *Exp. Biol.* **211**, 341-353.
598 **Fotowat, H. and Gabbiani, F.** (2007). Relationship between the phases of sensory and motor
599 activity during a looming-evoked multistage escape behavior. *J Neurosci* **27**(37), 1047-59.
600 **Fotowat, H. & Gabbiani, F.** (2011). Collision Detection as a Model for Sensory-Motor Integration.
601 *Annu. Rev. Neurosci.* 2011. **4**, 1–19.
602 **Fotowat, H., Harrison, R. and Gabbiani, F.** (2011). Multiplexing of Motor Information in the
603 Discharge of a Collision Detecting Neuron during Escape Behaviors. *Neuron* **69**, 147–158.
604 **Fry, S., Rohrseitz, N., Straw, A. and Dickinson, M.** (2009). Visual control of flight speed in
605 Drosophila melanogaster. *J. Exp Biol.* **212**, 1120-1130.
606 **Gabbiani, F., Krapp, HG. and Laurent, G.** (1999). Computation of object approach by a wide
607 field, motion-sensitive neuron. *J Neuroscience* **19**, 1122–1141.
608 **Glantz, R.M.** (1974) Defense reflex and motion detector responsiveness to approaching targets: the
609 motion detector trigger to the defense reflex pathway. *J Comp Physiol* **95**, 297.
610 **Gray, J. R., Lee, J. K. and Robertson, R. M.** (2001). Activity of descending contralateral
611 movement detector neurons and collision avoidance behaviour in response to head-on visual
612 stimuli in locust. *J. Comp. Physiol. A* **187**, 115-129.
613 **Hatsopoulos, N., Gabbiani, F. and Laurent, G.** (1995). Elementary computation of object approach
614 by wide-field visual neuron. *Science* **270**, 1000 –1003.
615 **Hemmi, J. M.** (2005a). Predator avoidance in fiddler crabs: 1. Escape decisions in relation to the risk
616 of predation. *Anim. Behav*. **69**, 603-614.

Hemmi, J. M. (2005b). Predatory avoidance in fiddler crab: 2. The visual cues. *Anim. Behav*. **69**, 615-625.

Hemmi, JM. and Tomsic D. (2011). The neuroethology of escape in crabs: from sensory ecology to neurons and back. *Current Opinion in Neurobiology*, **22**. 1–7.

Hemmi, J. M. and Zeil, J. (2005). Animals as prey: perceptual limitations and behavioral options. *Mar. Ecol. Prog. Ser*. **287**, 274-278.

Hemmi, J. M. & Pfeil, A. (2010). A multi-stage anti-predator response increases information on predation risk. *J. Exp. Biol.* **213**, 1484–1489.

Land, M. and Layne, J.E. (1995b). The visual control of behaviour in fiddler crabs. II. Tracking control systems in courtship and defence. *J Comp Physiol A* **177**, 91.

Liden, W. H. & Herberholz, J. (2008). Behavioral and neural responses of juvenile crayfish to moving shadows. *J. Exp. Biol*. **211**, 1355–1361.

Laurent G, Gabbiani F. (1998). Collision-avoidance: nature's many solutions. *Nat. Neurosci.* **1**, 261–63

Lee, D.N. (1980). The optic flow field: the foundation of vision. *Phil. Trans R.Coc. Lond. B* **290**, 169-179.

Medan, V., Oliva, D. and Tomsic, D. (2007). Characterization of Lobula Giant neurons responsive to visual stimuli that elicit escape reactions in the crab *Chasmagnathus*. *J. of Neurophysiology* **98**, 2414-2428.

Oliva, D., Medan, V. and Tomsic, D. (2007). Escape behaviour and neuronal responses to looming stimuli in the crab *Chasmagnathus granulatus* (Decapoda: Grapsidae). *J. Exp. Biol.* **210**, 865-880.

Oliva, D. (2010). Mechanisms of visual detection and avoidance of collision stimuli in a new experimental model, the crab *Chasmagnathus granulatus* PhD Thesis, University of Buenos Aires.

Preuss, T., Osei-Bonsu, PE., Weiss, SA., Wang, C. and Faber DS. (2006). Neural representation of object approach in a decision-making motor circuit. *J. Neurosci.* **26**, 3454–64.

Rind, F.C. and Simmons, P.J. (1999). Seeing what is coming: building collision-sensitive neurones. *Trends Neurosci* **22** (5), 215-20.

Santer, RD., Simmons, PJ. and Rind, FC. (2005a). Gliding behaviour elicited by lateral looming stimuli in flying locusts. *J. Comp. Physiol. A* **191**, 61–73.

Santer, RD., Yamawaki, Y., Rind, FC. and Simmons, PJ. (2005b). Motor activity and trajectory control during escape jumping in the locust *Locusta migratoria*. *J. Comp. Physiol. A* **191**, 965–75.

Santer, RD., Rind, FC., Stafford, R. and Simmons, PJ. (2006). Role of an identified looming-sensitive neuron in triggering a flying locust's escape. *J. Neurophysiol.* **95**, 3391–400.

Santer RD, Yamawaki Y, Rind FC. and Simmons, PJ. (2008). Preparing for escape: an examination of the role of the DCMD neuron in locust escape jumps. *J. Comp. Physiol. A* **194**, 69–77.

Sun, H. and Frost, B. (1998). Computation of different optical variables of looming objects in pigeon nucleus rotundus neurons. *Nature neuroscience.* **4**, 296-303.

Srinivasan, M.V., Zhang, S.W., Chahl, J.S., Barth, E. and Venkatesh, S. (2000). How honeybees make grazing landings on flat surfaces. Biological Cybernetics **83**, 171–183.

Sztarker, J. and Tomsic, D. (2008). Neuronal correlates of the visually elicited escape response of the crab Chasmagnathus upon seasonal variations, stimuli changes and perceptual alterations. *J Comp Physiol A* **194**(6), 587-96.

Tammero, L. F. and Dickinson, M. H. (2002). Collision-avoidance and landing responses are mediated by separate pathways in the fruit fly, *Drosophila melanogaster*. *J. Exp. Biol.*, **205**, 2785-2798.

Tomsic, D., Berón de Astrada, M. and Sztarker, J. (2003). Identification of individual neurons reflecting short- and long-term visual memory in an arthropod. *J Neurosci* **23**(24), 8539-46.

Wang, Y. and Frost, B. J. (1992). Time to collision is signalled by neurons in the nucleus rotundus of pigeons. Nature, **356**, 236-238.

Wasserman, L. (2004) All of Statistics. A concise course in Statistical inference. Springer. Chapter 8. pag. 107.

Wiersma, C. A. G., Roach J. L.M, and Glantz, R. M. (1982). Neural integration in the optic system. In: Sandeman DC, Atwood HL (eds). The biology of the Crustacea, vol 4. Neural integration and behavior. Academic Press, New York, pp 1–31

679 **FIGURE LEGENDS:**

680

681 **Figure 1.** (A) Measurement of the escape response. Locomotor activity was studied in a walking
682 simulator device which consisted of a styrofoam ball that could be freely rotated by the animal. The
683 crab was held in position by a weightless rod attached to its carapace that could slide up and down
684 within a guide located above the animal. Both the rod and the guide sleeve had square cross-sections,
685 which prevented the animal from rotating around its yaw axis. Locomotion was assessed by
686 recording the rotations of the ball with two mice as described elsewhere (Oliva et al., 2007). The ball
687 and the crab were surrounded by 5 screen monitors, each located at 20 cm from the animal. (B)
688 Simulation of an object's approach at constant speed. The right eye of the crab was stimulated from
689 the right side by presenting squares of half-size l approaching at a constant speed v toward the center
690 of the eye, at 90° relative to the animal's body axis. The figure shows the virtual object at two
691 different times during the simulated approach. $x(t)$ is the position of the object in a reference system
692 centered at the crab's right eye, $\theta(t)$ is the total subtended angle for the object at the crab's eye, and
693 l_{screen} is the half-size of the square drawn on the monitor screen.

694

695 **Figure 2.** Average instantaneous speed of escape to different stimuli. The lower part shows the
696 expansion dynamics for the 8 stimuli listed in Table 1. Above is the mean speed of the animals to
697 each stimulus, identified by a color code. Thin lines represent standard deviation of the mean. The
698 left part corresponds to stimuli number 1-4 in Table 1, which share the same speed but have different
699 sizes. The right part corresponds to stimuli 5-8, which share the same size but have different speeds.
700 Arrows below each trace mark mean escape initiation times (t_{esc}). Each animal received all the
701 stimuli, one every 3 min, in random order (N=20 animals). Notice the matching between stimulus
702 expansion dynamics and response performance throughout the stimuli. Dashed line rectangles
703 enclose the portion of the response corresponding to the time of stimulus expansion (used later in Fig.
704 11).

705

706 **Figure 3.** Representation of the measurement of an optical variable when the animal decides to
707 begin the escape run. (A) Speed of an individual response to a looming stimulus. (B) Angular size
708 $\theta(t)$ of the stimulus as a function of time. The optical variable (in this case angular size θ) should be
709 assessed at time t_{esc}-δ, where δ is the delay between the moment at which the animal decides to
710 escape and the associated measured response. The value of δ in the figure is drawn out of scale.

711

712 **Figure 4.** A) Estimation of the delay between the visual input and the motor output. The upper right
713 inset depicts the stimulus used for this experiment. It was a black edge of 60º height advancing on a
714 white background with constant angular velocity. The graph shows the latency between the start of

the stimulus movement and the measured response as a function of the stimulus angular velocity. The latency decreased with increasing stimulus speeds to a minimum asymptotic value of 170 ms. This value would correspond to the minimum time required to convey visual information downstream towards the motor system and move the walking device. A realistic estimate of δ, however, must also consider the time elapsed between the moment when the visual information reaches the retina and the moment when the decision is made (see further explanations in the text). B)

Figure 5. Stimulus optical variables and the decision to escape. We analyzed whether any of the variables $Z_{1\text{-}6}(t_{esc}\text{-}\delta)$ described in Table 2 attained a constant value with all the stimuli when animals decided to initiate the escape run. Out of the six variables analyzed, *angular increment* was the only one whose value remained constant throughout the different stimuli (p = 0.6). On average, crabs made the decision to escape when the apparent size of the stimulus increased beyond 7 ± 0.3 degrees (mean ± s.e; dashed line in the lower right panel of Fig. 5F).

Figure 6: Correlation between stimulus *l/v* and five kinematic variables as a function of time. Twenty crabs were presented with the 8 looming stimuli with different *l/v* values reported in Table 1 (one trial per stimulus and per crab). Correlation coefficients between *l/v* and instantaneous angular size, increment, velocity, acceleration, and time to collision were computed in 10ms steps. The only kinematic stimulus variable that crosses the zero correlation level within the time window expected for a functional delay is *angular increment*. See the text for details.

Figure 7. The escape run is under continuous visual regulation. To investigate the dependency of the escape speed on the incoming visual information, we performed an experiment using the same looming dynamics (*l=17 cm, v=71.5 cm/s)*, but stopping its expansion at different angular sizes (θ_{max} *= 23º, 34 º, 44º, 54 º, 62 º).* Traces show average speed of animals in response to the five stimuli shown below. Note that immediately after the stimulus stopped growing, the escape run always decelerated. Each stimulus was applied twice to each animal (N=6 animals).

Figure 8. Diagram that illustrates the escape response model using a phenomenological input-output relation f_{IO}. To attempt to characterize the escape response within each trial, we used a model described by the input-output relation given by $v_c(t)=f_{IO}[u_1(t\text{-}\delta)]$. (A) Stimulus angular increment $\Delta\theta$ as a function of time. (B) Input optical variable $u_1(t\text{-}\delta)=\Delta\theta(t\text{-}\delta)\text{-}\Delta\theta_{esc}$ as a function of time. This variable allowed us to determine whether the animal was still ($u_1<0$, blue circle), the time of the escape decision ($u_1=0$, green circle) or if the animal was escaping ($u_1> 0$, red circle). (C) The variable u_1 was inserted in the input-output relation f_{IO}, which provided the predicted animal's speed v_c. Note that f_{IO} depends on the value of $\Delta\theta_{esc}$, $v_{1,max}$ and $u_{1,50\%}$. Besides, f_{IO} is also characterized by

its slope at $u_1=0$. The slope, called m_1, depends on $v_{1,max}$ and $u_{1,50\%}$ as follows: $m_1 = v_{1,max} / u_{1,50}$.
(D) Prediction of the animal's speed as a function of time using the f_{IO} model. See text for further explanations.

Figure 9. (A) Example of escape response fits using the input-output relation $v_c = f_{IO}[u_1]$, for the 8 stimuli in a single crab. Fits were made for the time interval ranging from t_{esc} to the end of the expansion. For each record t_{esc} was determined as explained in methods, then we obtained $\Delta\theta_{esc}$ and, finally, $u_1(t-\delta)=\Delta\theta(t-\delta)-\Delta\theta_{esc}$ was calculated. The parameters of f_{IO} ($v_{1,max}$, $u_{1,50\%}$) were determined by least-square regression for each record using Eqn 6. Left and right panels show fits of responses to stimuli 1-4 and 5-8 of Table 1, respectively. Responses were individually fitted for all the animals (N = 20 animals, 8 stimuli per animal). (B-D) Values of $v_{1,max}$, $u_{1,50\%}$ and m_1 obtained after fitting the input-output relation $v_c = f_{IO}[u_1]$ for all trials. After obtaining f_{IO} using u_1 (Eqn 6), we tested whether $v_{1,max}$, $u_{1,50\%}$ and m_1 remained constant throughout the stimuli. As shown in panels A-C, the analyses revealed significant differences for the three parameters.

Figure 10. (A) Example of escape response fits using the input-output relation $v_c = f_{IO}[u_2]$, for the 8 stimuli in a single crab. Fits were made for the time interval ranging from t_{esc} to the end of the expansion. For each record t_{esc} was determined as explained in methods, then we obtained $\Delta\theta_{esc}$ and, finally, $u_2(t-\delta)$ was calculated. The parameters of f_{IO} ($v_{2,max}$, $u_{2,50\%}$) were determined by least-square regression for each record using Eqn 7. Left and right panels show fits of responses to stimuli 1-4 and 5-8 of Table 1, respectively. Responses were individually fitted for all the animals (N = 20 animals, 8 stimuli per animal).
(B-C) Values for $v_{2,max}$, $u_{2,50\%}$ and m_2 obtained by fitting the input-output relation $v_c = f_{IO}[u_2]$ for all trials. After obtaining f_{IO} using u_2 (Eqn 7), we tested whether $v_{2,max}$, $u_{2,50\%}$ and m_2 remained constant throughout the stimuli. As shown in panels A-C, the analyses did not reveal significant differences for any of the three parameters.

Figure 11. Average speed and predicted speed responses using the input-output relation $v_c = f_{IO}[u_2]$ (Eqn 8). The curves illustrate the segment of data of Fig. 2, corresponding to the time of stimulus expansion (dashed line rectangles in Fig 2). Mean speed response values (in color) and predicted speed (black traces) for all the tested stimuli (left: stimuli 1-4 of table 1, right: stimuli 5-8). The predicted values were obtained by using the proposed input-output relation $v_c=f_{IO}[u_2]$, with mean parameters' values estimated from experimental data ($\Delta\theta_{esc}=7^o$, $v_{2,max}=17$ cm/s, and $u_{2,50\%}=490$ deg^2 /s).

TABLE LEGENDS:

Table 1. Parameters of looming stimuli (see Fig. 1B). l is the half-size of the object, v is the approach speed, L is the initial distance and θ_0 is the initial angular size of the object.

Table 2. Variables Z that animals could compute to decide to start an escape run.

Figure 1

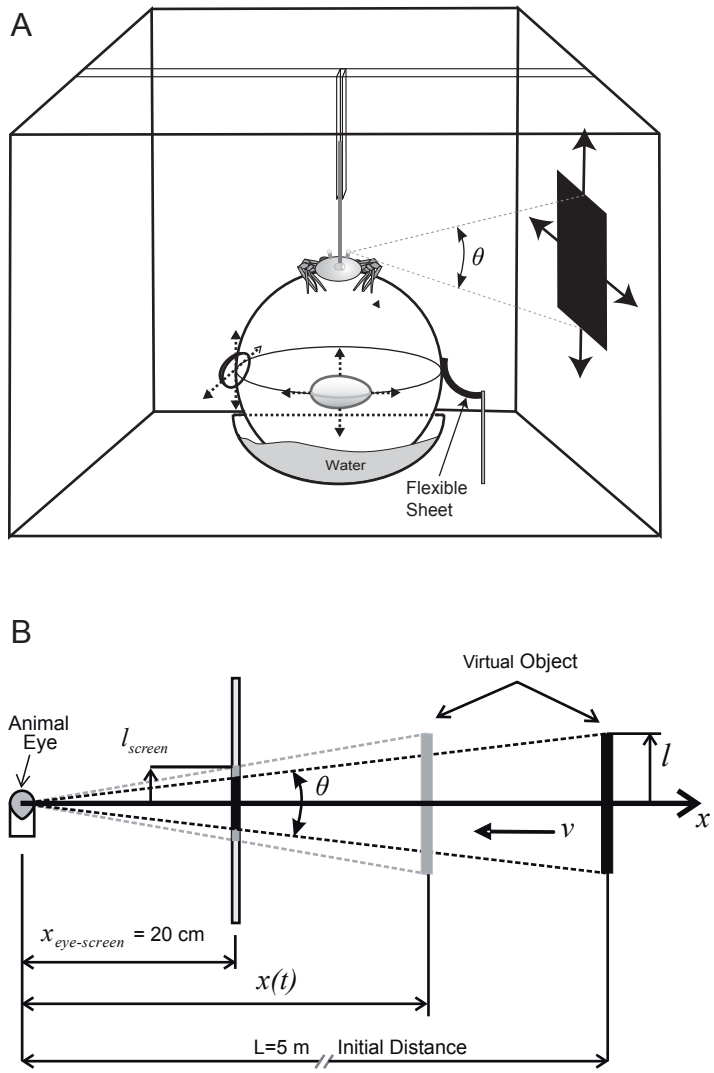

Figure 2

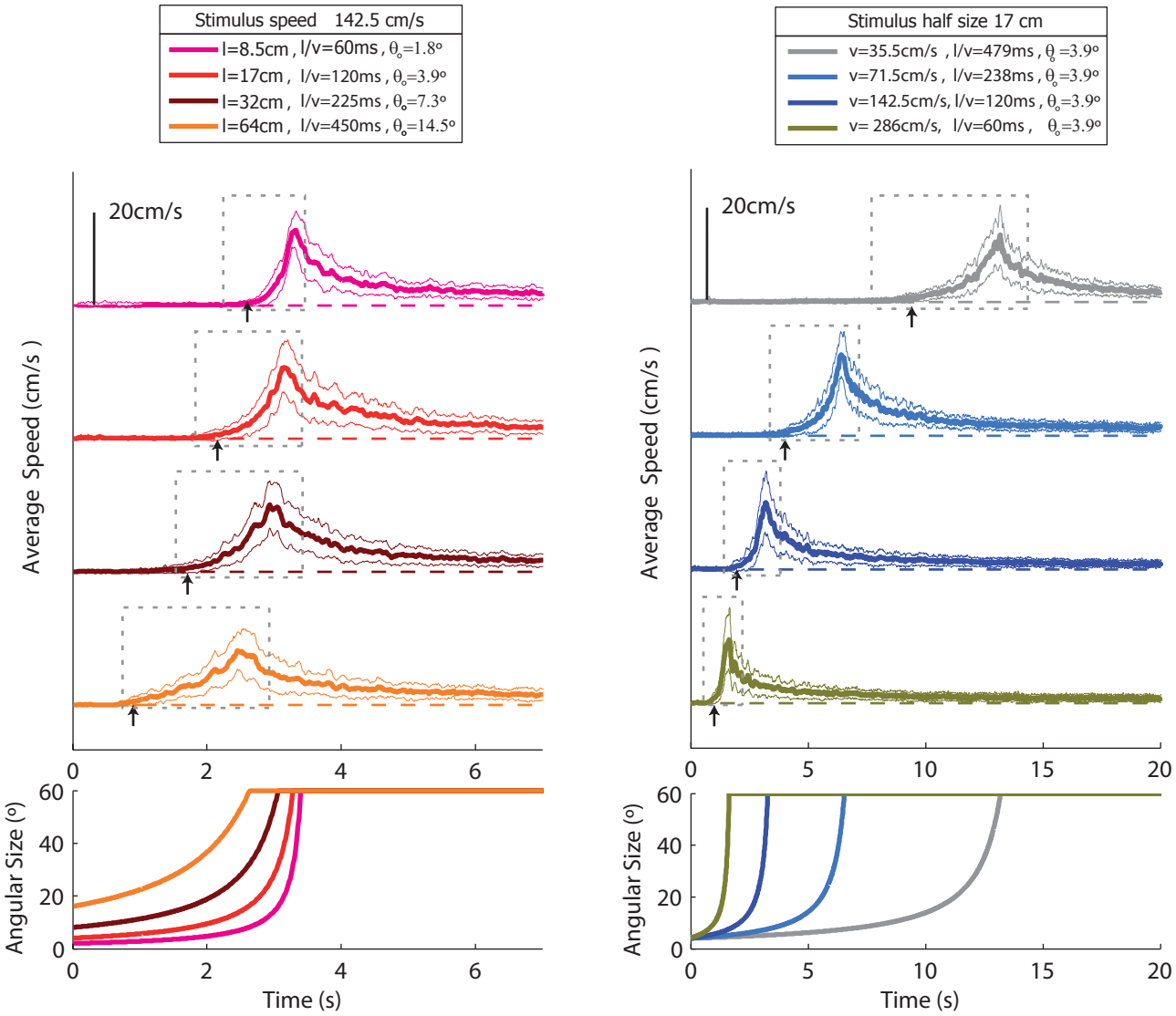

Figure 3

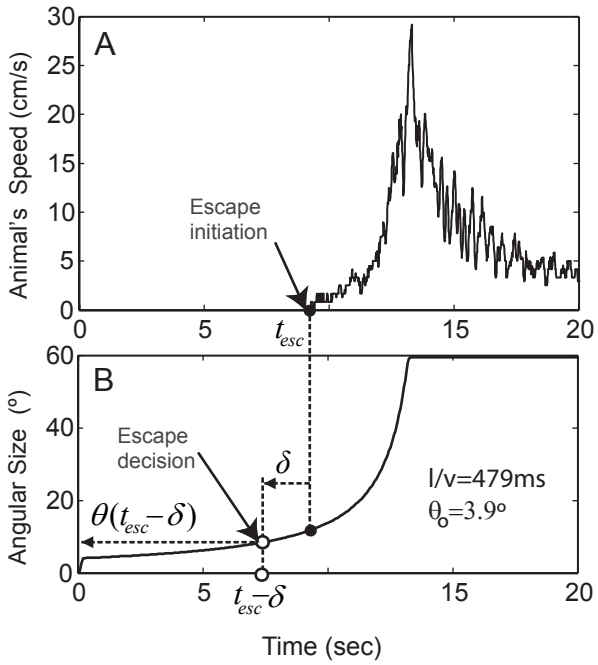

Figure 4

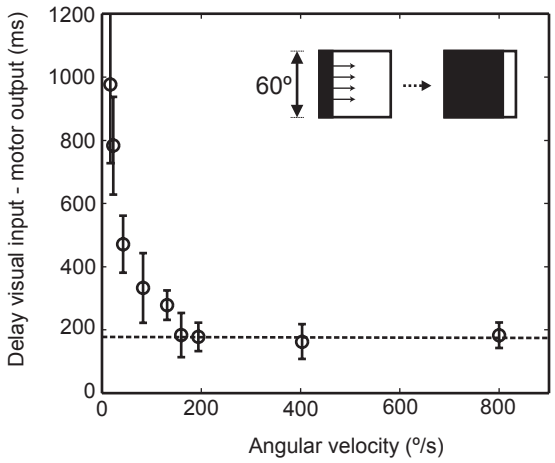

Figure 5

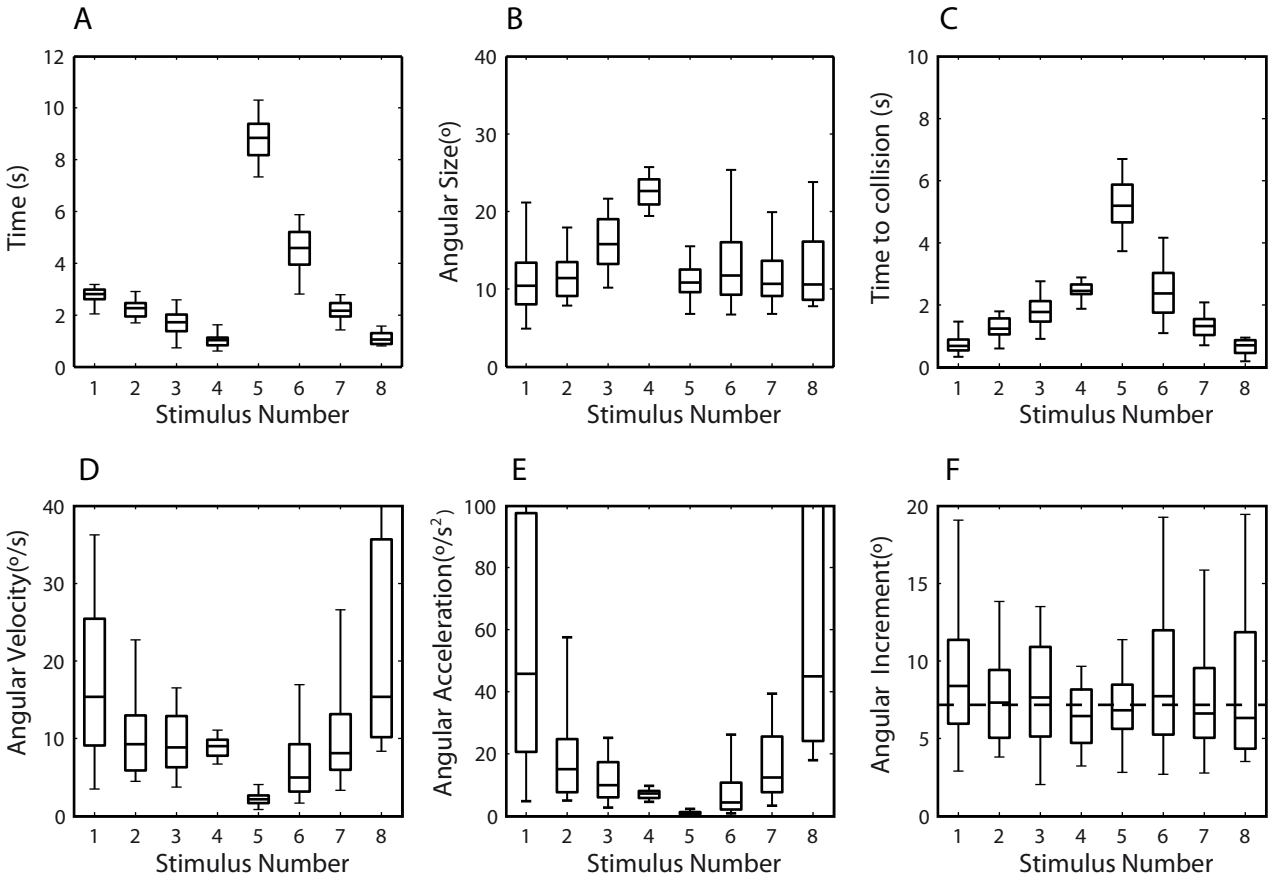

Figure 6

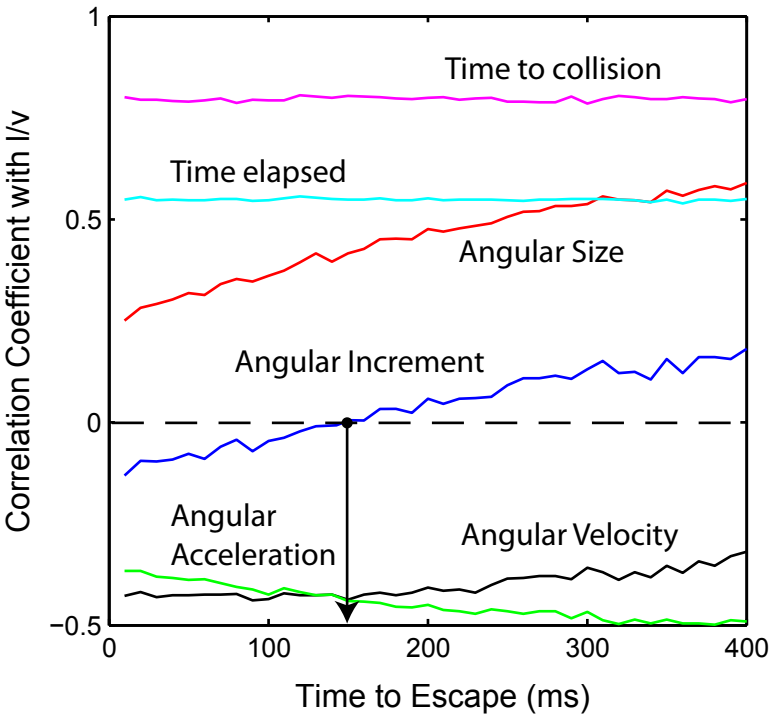

Figure 7

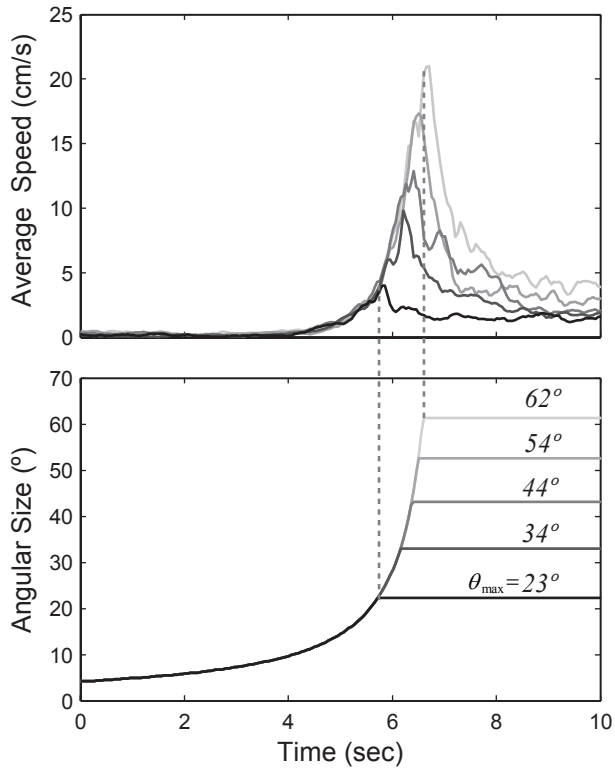

Figure 8

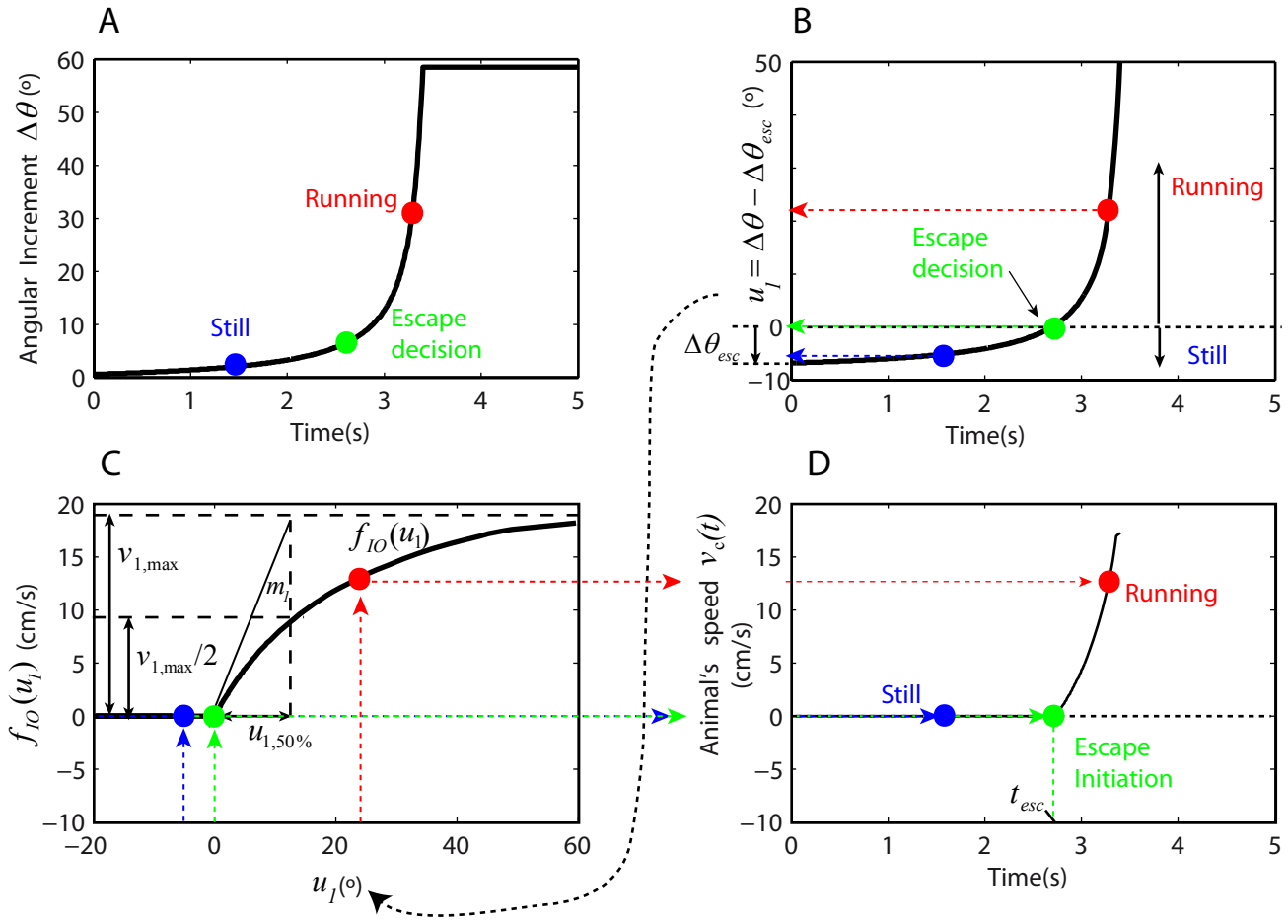

Figure 9

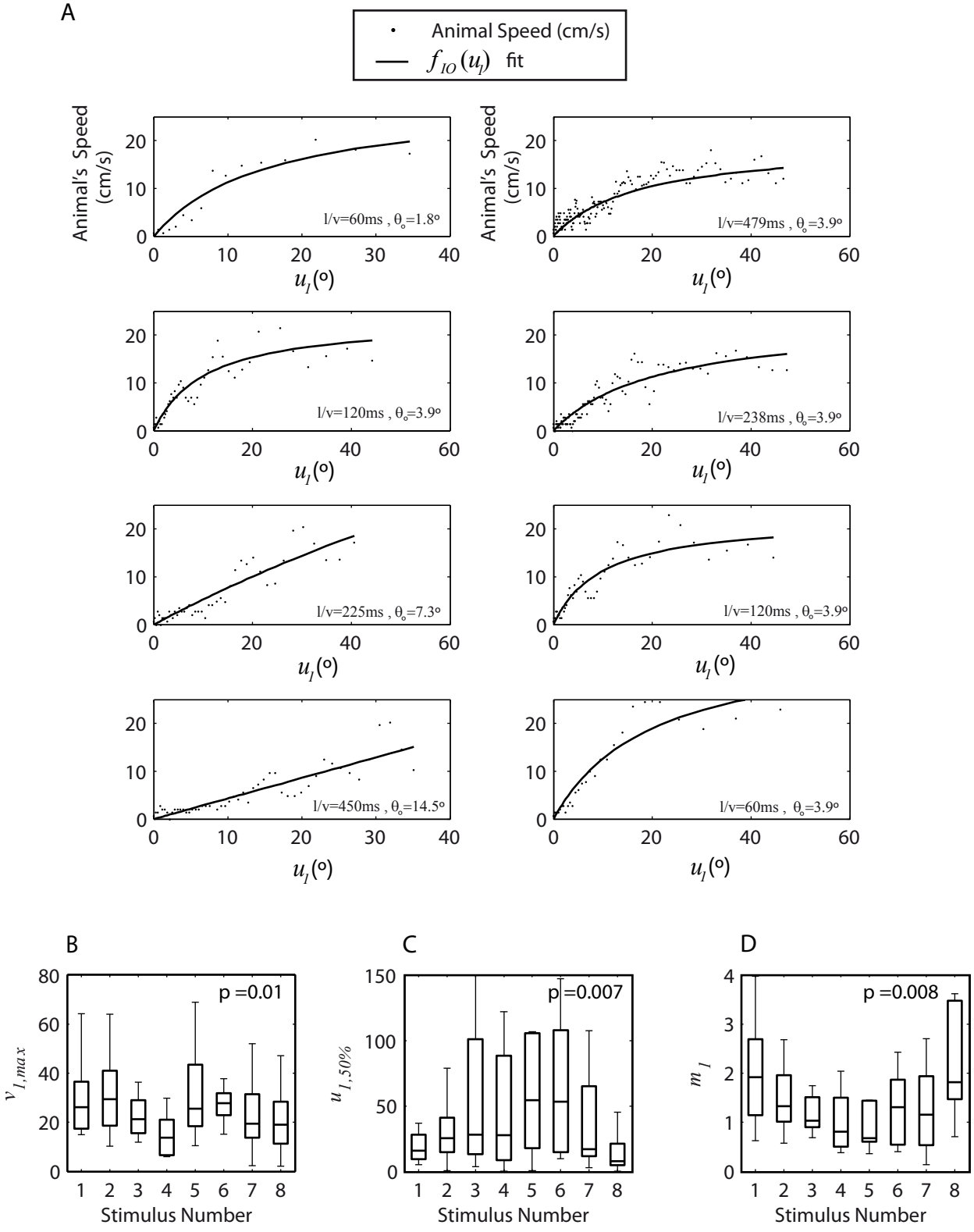

Figure 10

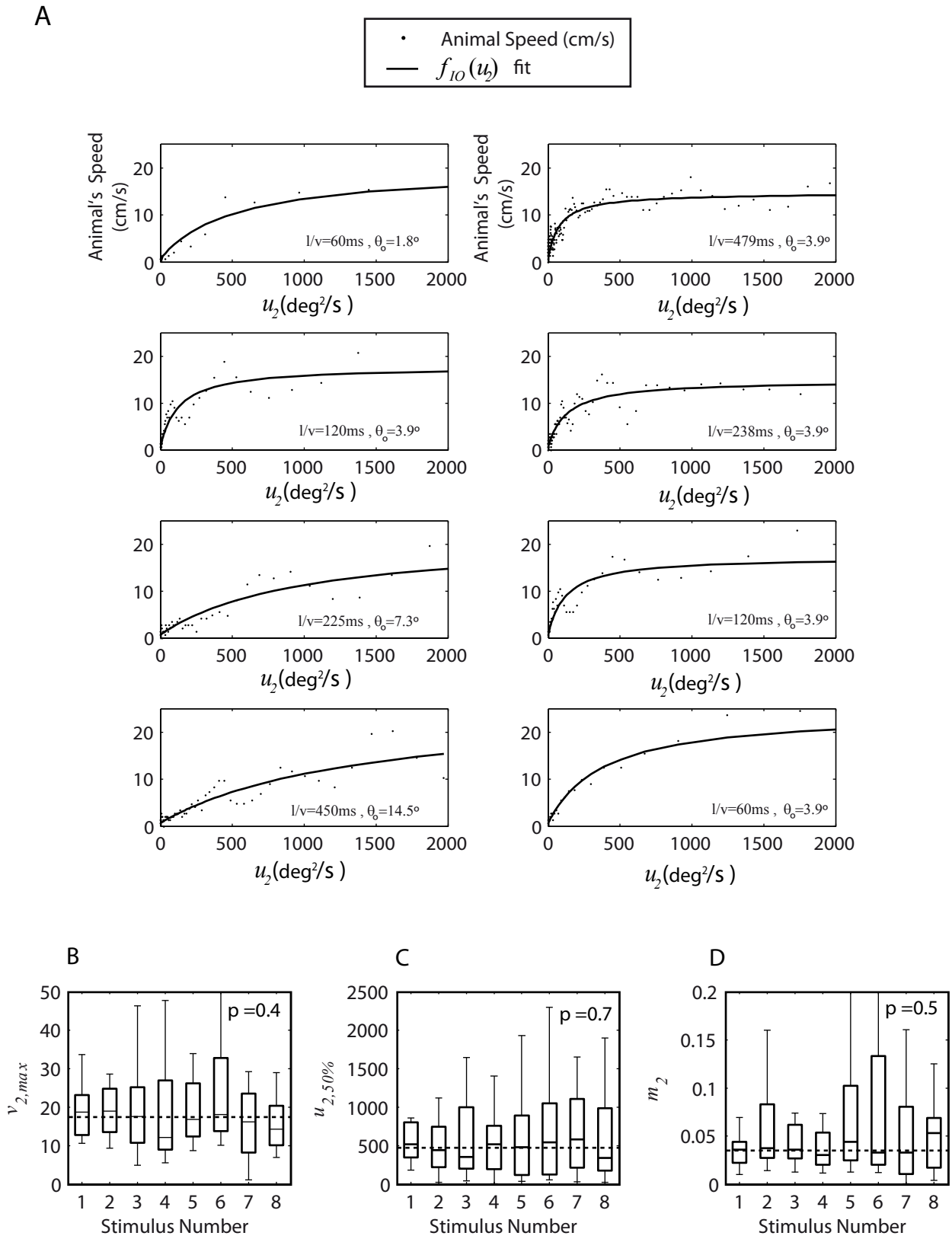

Figure 11

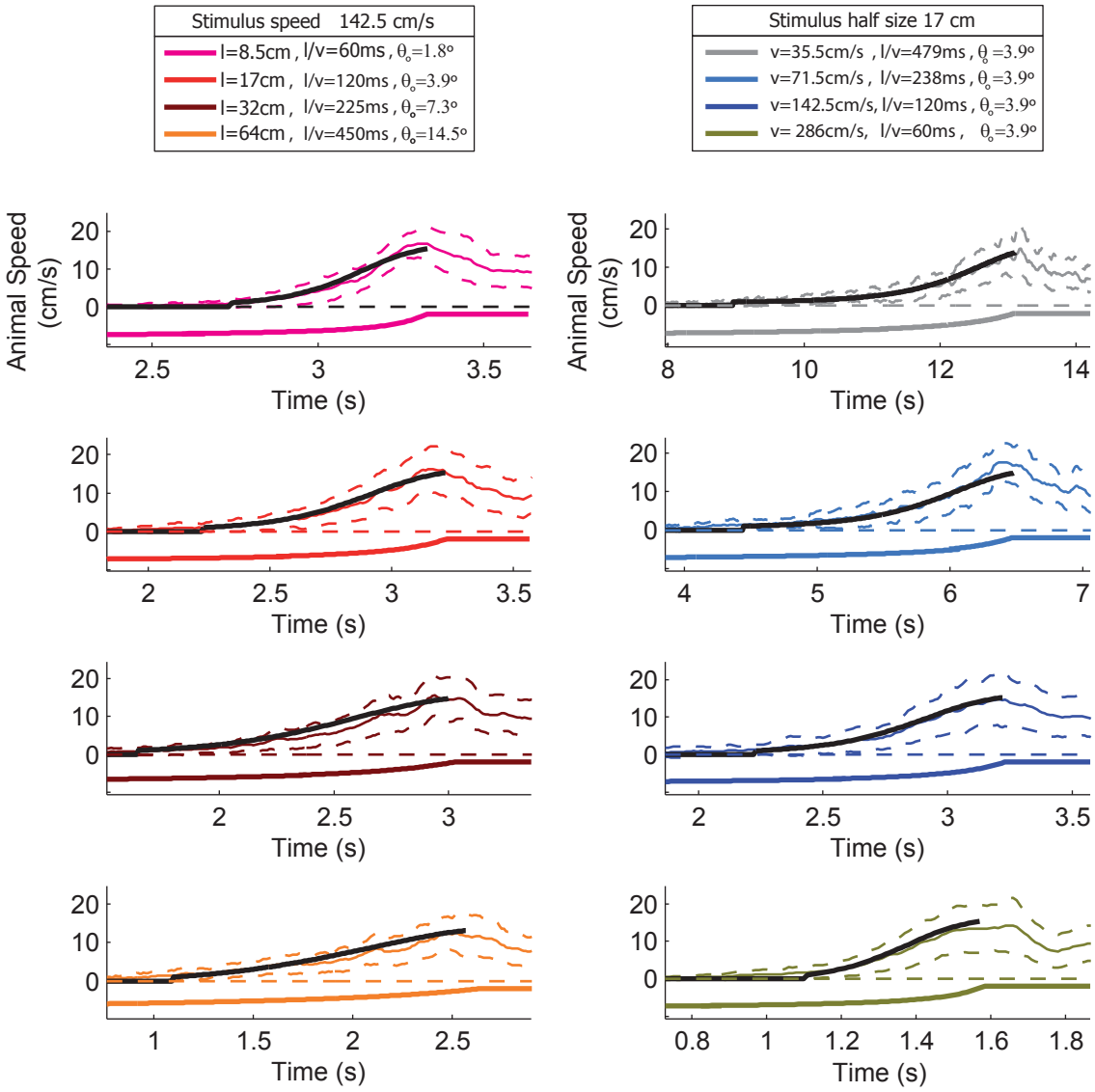

Table 1

Stimulus Number	***l*(cm)**	***v*** **cm/s**	***l/v*** **(ms)**	**L (m)**	**T (s)**	θ_0 **(deg.)**
1	8.5	142.5	60	5	3.5	1.8
2	17	142.5	120	5	3.5	3.9
3	32	142.5	225	5	3.5	7.3
4	64	142.5	450	5	3.5	14.5
5	17	35.5	479	5	14	3.9
6	17	71.5	238	5	7	3.9
7	17	142.5	120	5	3.5	3.9
8	17	286	60	5	1.75	3.9

Table 1. Parameters of looming stimuli (see Fig. 1B). l is the half-size of the object, v is the approach speed, L is the initial distance and θ_0 is the initial angular size of the object.

Table 2

Variable	Notation	Description
Z_1	t_{esc}	Elapsed Time
Z_2	t_c.	Time to collision
Z_3	θ	Angular Size
Z_4	$\dot{\theta}$	Angular Velocity
Z_5	$\ddot{\theta}$	Angular Acceleration
Z_6	$\Delta\theta$	Angular Increment

Table 2. Variables *Z* that animals could compute to decide to start an escape run.